ARMY RESEARCH LABORATORY

Toward Improving the Efficiency and Realism of Coupled Meteorological—Acoustic Computer Models for the Forest Canopy

by Arnold Tunick

ARL-MR-586 April 2004

NOTICES

Disclaimers

The findings in this report are not to be construed as an official Department of the Army position unless so designated by other authorized documents.

Citation of manufacturer's or trade names does not constitute an official endorsement or approval of the use thereof.

Destroy this report when it is no longer needed. Do not return it to the originator.

Army Research Laboratory
Adelphi, MD 20783-1197

ARL-MR-586 **April 2004**

Toward Improving the Efficiency and Realism of Coupled Meteorological—Acoustic Computer Models for the Forest Canopy

Arnold Tunick
Computational and Information Sciences Directorate, ARL

REPORT DOCUMENTATION PAGE

Form Approved
OMB No. 0704-0188

1. REPORT DATE *(DD-MM-YYYY)*	2. REPORT TYPE	3. DATES COVERED (From - To)
April 2004	Final	July 2003–March 2004

4. TITLE AND SUBTITLE
Toward Improving the Efficiency and Realism of Coupled Meteorological—Acoustic Computer Models for the Forest Canopy

5a. CONTRACT NUMBER

5b. GRANT NUMBER

5c. PROGRAM ELEMENT NUMBER

6. AUTHOR(S)
Arnold Tunick

5d. PROJECT NUMBER

5e. TASK NUMBER

5f. WORK UNIT NUMBER

7. PERFORMING ORGANIZATION NAME(S) AND ADDRESS(ES)
U.S. Army Research Laboratory
ATTN: AMSRD-ARL-CI-EE
2800 Powder Mill Road
Adelphi, MD 20783-1197

8. PERFORMING ORGANIZATION REPORT NUMBER
ARL-MR-586

9. SPONSORING/MONITORING AGENCY NAME(S) AND ADDRESS(ES)
U.S. Army Research Laboratory
2800 Powder Mill Road
Adelphi, MD 20783-1197

10. SPONSOR/MONITOR'S ACRONYM(S)

11. SPONSOR/MONITOR'S REPORT NUMBER(S)

12. DISTRIBUTION/AVAILABILITY STATEMENT
Approved for public release; distribution unlimited.

13. SUPPLEMENTARY NOTES

14. ABSTRACT

Several physics-based computer models have been developed to calculate one- and two-dimensional forest canopy micrometeorology and turbulence for future U.S. Army acoustic application research. Individual computer codes have incorporated various computational methods on a uniform grid to solve the meteorological fields. However, it may be possible to improve the efficiency and realism of the coupled meteorological—acoustic computer models by introducing variable grid. Variable grid will allow for better distribution of grid points and will extend calculations higher into the boundary layer above the forest. A finer grid inside the forest and a coarser grid above the forest will help to resolve important meteorological (and acoustic) scales and processes.

Therefore, the following report presents results from some preliminary tests to incorporate this important feature into numerical codes. First, several simpler physics-based diffusion models are developed to benchmark fundamental (numerical) techniques. Both explicit and implicit differencing schemes are examined. In addition, numerical stability criteria for these calculations are demonstrated. Then, successful preliminary tests on these codes are extended to more complicated meteorological—acoustic models for the forest canopy.

15. SUBJECT TERMS
conservation equations, numerical methods, numerical stability, computer model

16. SECURITY CLASSIFICATION OF:			17. LIMITATION OF ABSTRACT	18. NUMBER OF PAGES	19a. NAME OF RESPONSIBLE PERSON
a. REPORT	b. ABSTRACT	c. THIS PAGE			Arnold Tunick
Unclassified	Unclassified	Unclassified	UL	24	19b. TELEPHONE NUMBER (*Include area code*) 301-394-1765

Standard Form 298 (Rev. 8/98)
Prescribed by ANSI Std. Z39.18

Contents

List of Figures

Acknowledgments

The author gratefully acknowledges Ronald Meyers, David Rosen, and Keith Deacon of the U.S. Army Research Laboratory for offering helpful comments on numerical methods and stability analysis.

1. Introduction

The U.S. Army has a growing interest in the use of advanced sensors and computer models to retrieve, display, and interpret acoustic signals on future battlefields. Such technologies are emerging for the surveillance, detection, identification, and tracking of sound-emitting targets in and around forests, hilly terrain, and in cities (*1*). Consequently, the U.S. Army is looking to implement the best possible computer models for determining point-to-point acoustic transmission. At the same time, the retrieval and interpretation of acoustic signals are greatly influenced by turbulence and refraction effects caused by finer scale atmospheric motions over varying topography and surface energy budgets (*2*). Hence, improved physics-based theory and computer models for meteorology coupled to acoustics are expected to contribute important information on the performance of future combat (acoustic) systems.

Recently, several physics-based computer models have been developed to calculate one- and two-dimensional forest canopy micrometeorology and turbulence for future U.S. Army acoustic application research (*3, 4*). Individual computer codes have incorporated various computational schemes on a uniform grid to solve the meteorological fields (*5*). However, it may be possible to improve the efficiency and realism of the coupled meteorological—acoustic computer models by introducing variable grid. Variable grid will allow for better distribution of grid points and will extend calculations higher into the boundary layer above the forest. In addition, a finer grid inside the forest and a coarser grid above the forest will help to resolve important meteorological (and acoustic) scales and processes.

Thus, the following report presents results from some preliminary tests to incorporate this important feature into numerical codes. First, several simpler diffusion models are developed to benchmark fundamental (numerical) techniques. Both explicit and implicit differencing schemes are examined. In addition, numerical stability criteria for these calculations are demonstrated. Then, successful preliminary tests on these codes are extended to more complicated meteorological—acoustic models for the forest canopy.

2. Explicit Differencing

A simplified conservation equation to describe the mean concentration (diffusion) of a scalar $\overline{C}$ can be written as follows:

$$\frac{\partial \overline{C}}{\partial t} = -\overline{u}\frac{\partial \overline{C}}{\partial x} - \frac{\partial \overline{w'C'}}{\partial z} \quad , \tag{1}$$

where t is the independent variable time, $\overline{u}$ is the mean longitudinal component of the wind velocity, x is range, z is height above ground, and $\overline{w'C'}$ is the mean scalar flux. The flux-gradient assumption (*6*) suggests that

$$-\overline{w'C'} = K\frac{\partial \overline{C}}{\partial z} \quad , \tag{2}$$

where K is the scalar (eddy) diffusivity. Combining equations 1 and 2 yields,

$$\frac{\partial \overline{C}}{\partial t} = -\overline{u}\frac{\partial \overline{C}}{\partial x} + K\frac{\partial^2 \overline{C}}{\partial z^2} \quad . \tag{3}$$

In discretized form, this simple model can be solved forward in time using the following explicit differencing scheme for variable grid, i.e.,

$$\overline{C}_{i,j}^{n+1} = \overline{C}_{i,j}^{n} + \Delta t\left[-\overline{u}_{i,j}\frac{\overline{C}_{i,j}^{n} - \overline{C}_{i-1,j}^{n}}{x_i - x_{i-1}} + K\frac{\overline{C}_{i,j+1}^{n}(z_j - z_{j-1}) + \overline{C}_{i,j-1}^{n}(z_{j+1} - z_j) - \overline{C}_{i,j}^{n}(z_{j+1} - z_{j-1})}{\tfrac{1}{2}(z_{j+1} - z_{j-1})(z_{j+1} - z_j)(z_j - z_{j-1})}\right], \tag{4}$$

where i and j are the indices for the horizontal and vertical grid, respectively, and n is the time-step. To execute the model, the following steps may be taken:

1. Initialize the scalar field as $C_{i,j}^{1} = e^{\frac{-(z-h)^2}{2\sigma^2}}$, where h defines the center and σ defines the width of the Gaussian profile.
2. Assume the wind flow is constant, i.e., $\overline{u}_{i,j} = 3.0\ ms^{-1}$.
3. Let the horizontal grid be constant, i.e., $\Delta x = 0.5\ m$.
4. Assume horizontal scalar gradients are zero, i.e., apply the explicit boundary condition $\overline{C}_{2,j}^{n} = \overline{C}_{1,j}^{n}$ at the upstream lateral edge.
5. Implement the following variable grid:

$$\Delta z = 0.25\ m \qquad 0.25 < z \leq 10.0\ m \ ,$$

$$\Delta z = 0.50\ m \qquad 10.5 < z \leq 30.0\ m \ ,$$

$$\Delta z = 1.00\ m \qquad 31.0 < z \leq 50.0\ m \ .$$

Figure 1 shows the model results for the case where the scalar diffusivity is $K = 10\ m^2\ s^{-1}$ and the time-step is $\Delta t = 0.001\ s$. These are the time-height contours derived from a simple scalar diffusion model solved via an explicit differencing scheme. Here, the time-step is small to satisfy the stability criterion described by Press et al. (*7*) as

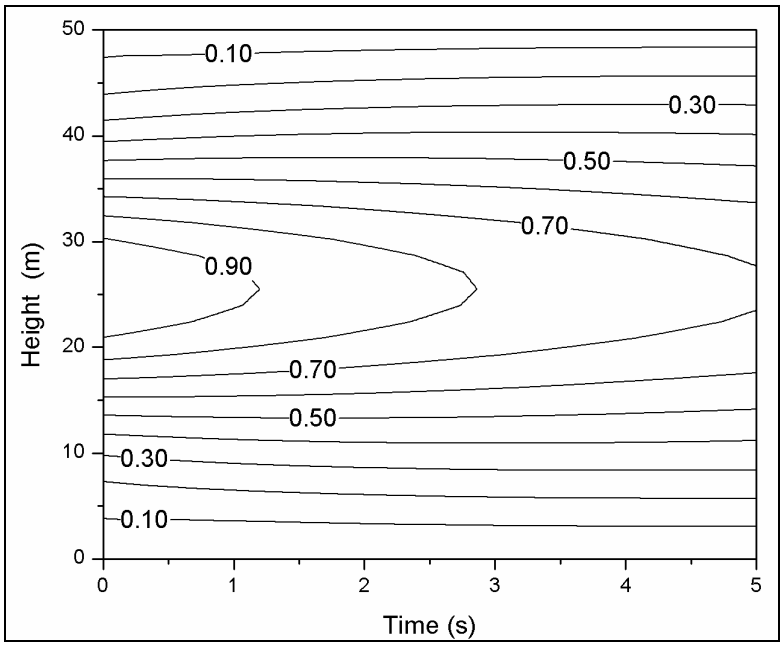

Figure 1. Time-height contours derived from a scalar diffusion model solved via an explicit differencing scheme. In this example, the scalar diffusivity is $K = 10\ m^2\ s^{-1}$ and the time-step is $\Delta t = 0.001\ s$.

$$\frac{2K\Delta t}{(\Delta z)^2} < 1 \quad . \tag{5}$$

Otherwise, for larger time-steps, the numerical scheme would be unstable and the model would not produce viable results. Alternately, figure 2 shows several profiles of scalar concentration at different time-steps derived from this model. Finally, for comparison, figure 3 shows the time-height contours for the case where $K = 3\ m^2\ s^{-1}$ and the time-step is $\Delta t = 0.01\ s$.

3. Time-Dependent Implicit Differencing

Alternately, equation 3 (without advection) can be solved via implicit differencing. The discretized form for equation 3 in this case can be written as

$$\overline{C}_{i,j}^{n+1} - \overline{C}_{i,j}^{n} = K\Delta t\left[\frac{\overline{C}_{i,j+1}^{n+1}\left(z_j - z_{j-1}\right) + \overline{C}_{i,j-1}^{n+1}\left(z_{j+1} - z_j\right) - \overline{C}_{i,j}^{n+1}\left(z_{j+1} - z_{j-1}\right)}{\tfrac{1}{2}\left(z_{j+1} - z_{j-1}\right)\left(z_{j+1} - z_j\right)\left(z_j - z_{j-1}\right)}\right] \quad . \tag{6}$$

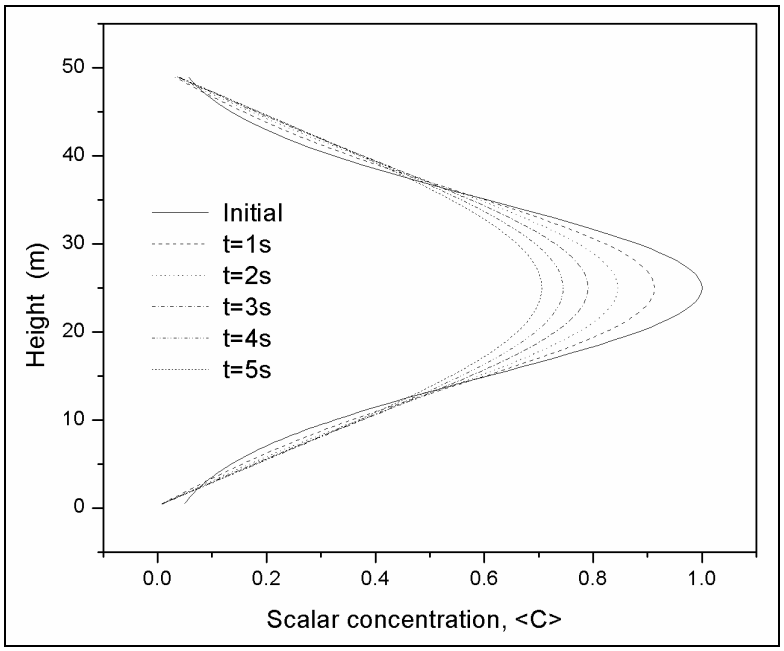

Figure 2. Time-dependent profiles of scalar concentration derived from a scalar diffusion model solved via an explicit differencing scheme.

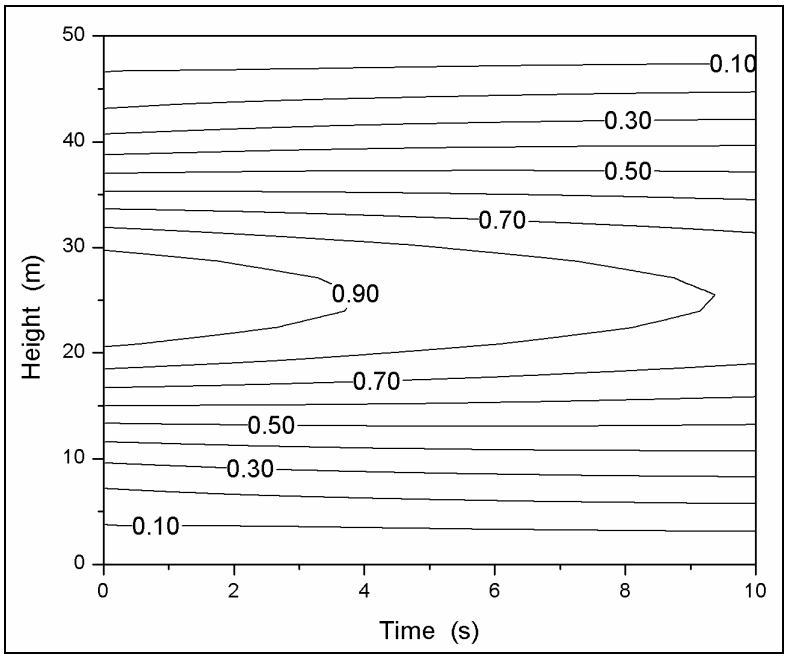

Figure 3. Same as figure 1 except the scalar diffusivity $K = 3\ m^2\ s^{-1}$ and the time-step is $\Delta t = 0.01\ s$.

If it is assumed that

$$\alpha = \frac{K\Delta t}{\frac{1}{2}\left(z_{j+1} - z_{j-1}\right)\left(z_{j+1} - z_{j}\right)\left(z_{j} - z_{j-1}\right)} \quad , \tag{7}$$

then equation 6 can be solved for $\overline{C}_{i,j}^{n}$ as

$$-\alpha\left(z_j - z_{j-1}\right)\,\overline{C}_{i,j+1}^{n+1} + \left[1 + \alpha\left(z_{j+1} - z_{j-1}\right)\right]\,\overline{C}_{i,j}^{n+1} - \alpha\left(z_{j+1} - z_j\right)\,\overline{C}_{i,j-1}^{n+1} = \overline{C}_{i,j}^{n} \quad . \tag{8}$$

Now, equation 8 can be solved via a tridiagonal matrix algorithm (also called the Thomas algorithm) (Press et al. [*8*]). By implementing the Thomas algorithm, one is looking for a solution to the equation **A** · **x** = **r**, which can be written in matrix-vector notation as

$$\begin{bmatrix} b_1 & c_1 & 0 & \ldots & & & \\ a_2 & b_2 & c_2 & \ldots & & & \\ & & & \ldots & & & \\ & & & \ldots & a_{N-1} & b_{N-1} & c_{N-1} \\ & & & \ldots & 0 & a_N & b_N \end{bmatrix} \cdot \begin{bmatrix} x_1 \\ x_2 \\ \ldots \\ x_{N-1} \\ x_N \end{bmatrix} = \begin{bmatrix} r_1 \\ r_2 \\ \ldots \\ r_{N-1} \\ r_N \end{bmatrix} \quad . \tag{9}$$

Here **a**, **b**, **c**, and **r** are the input vectors and **x** is the (scalar) output vector. The sub-, main-, and super-diagonal vectors (**a**, **b**, and **c**, respectively) can be computed from equation 8 as

$$a_{i,j} = -\alpha\left(z_{j+1} - z_j\right) \quad , \tag{10}$$

$$b_{i,j} = 1 + \alpha\left(z_{j+1} - z_{j-1}\right) \quad , \tag{11}$$

and

$$c_{i,j} = -\alpha\left(z_j - z_{j-1}\right) \quad . \tag{12}$$

The input vector **r** is defined as,

$$r_{i,j} = \overline{C}_{i,j}^{n} \quad . \tag{13}$$

In addition, the following boundary conditions are implemented: at z_1, $a_{i,1} = 0$, $b_{i,1} = 1$, $c_{i,1} = 0$, and $r_{i,1} = \overline{C}_{i,1}$ and at z_N, $a_{i,N} = 0$, $b_{i,N} = 1$, $c_{i,N} = 0$, and $r_{i,N} = \overline{C}_{i,N}$.

Figure 4 shows the time-height contours derived from this scalar diffusion model solved via implicit differencing, where the scalar diffusivity is $K = 10\ m^2\ s^{-1}$ and the time-step is $\Delta t = 0.1\ s$. As expected, these results are quite similar to those shown earlier derived via explicit differencing (figure 1). Except here, the magnitude of the time-step is not critical because the stability criterion for this model is given instead as

$$\frac{1}{1+\frac{4K\Delta t}{(\Delta z)^2}} < 1 \quad , \tag{14}$$

so that the numerical scheme is unconditionally stable for both large and small Δt (*9*). Alternately, figures 5 and 6 show, for comparison, the time-height contours for the case where Δt = 0.5 *s* and Δt = 1.0 *s*, respectively.

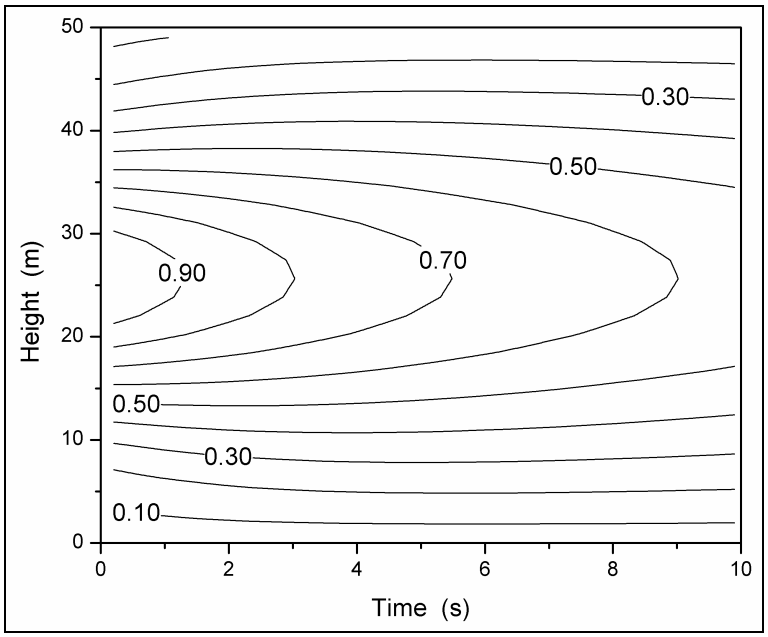

Figure 4. Time-height contours derived from a scalar diffusion model solved via an implicit differencing scheme. In this example, the scalar diffusivity is $K = 10\ m^2\ s^{-1}$ and the time-step is $\Delta t = 0.1\ s$.

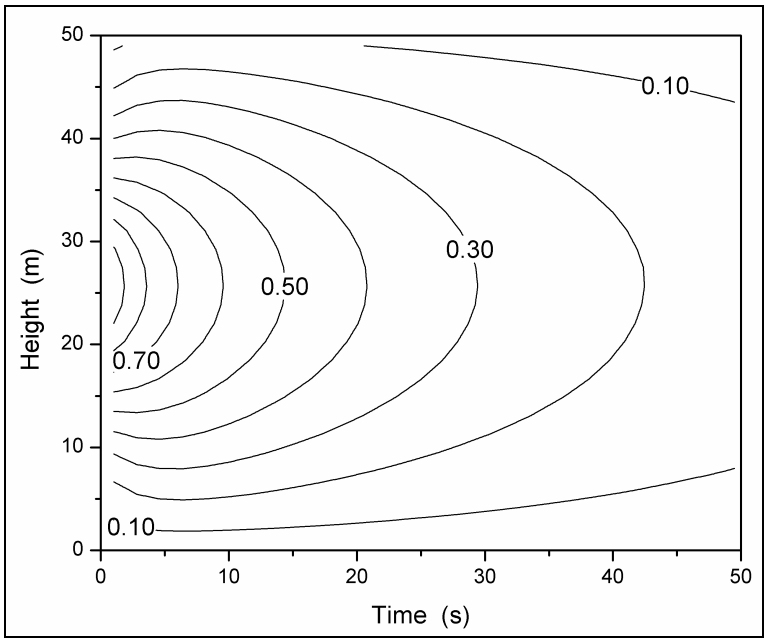

Figure 5. Same as figure 4 except the time-step is $\Delta t = 0.5\ s$.

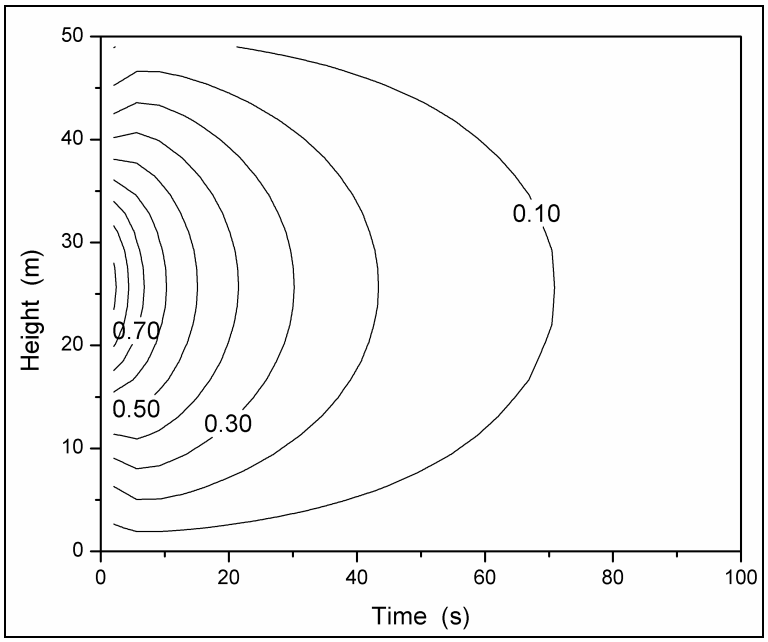

Figure 6. Same as figure 4 except the time-step is $\Delta t = 1.0\ s$.

4. Steady-State Implicit Differencing

4.1 Scalar Diffusion Model

In contrast, a steady-state model can be derived from equation 3, i.e.,

$$\frac{d^2\overline{C}}{dz^2} = \frac{\overline{u}}{K}\frac{d\overline{C}}{dx} \quad , \tag{15}$$

which can be written in discretized form as,

$$\frac{\overline{C}_{i,j+1}\left(z_j - z_{j-1}\right) + \overline{C}_{i,j-1}\left(z_{j+1} - z_j\right) - \overline{C}_{i,j}\left(z_{j+1} - z_{j-1}\right)}{\tfrac{1}{2}\left(z_{j+1} - z_{j-1}\right)\left(z_{j+1} - z_j\right)\left(z_j - z_{j-1}\right)} = \frac{\overline{u}_{i,j}}{K}\frac{\overline{C}_{i,j} - \overline{C}_{i-1,j}}{x_i - x_{i-1}} \quad . \tag{16}$$

If it is assumed that

$$\alpha = \frac{K\Delta x}{\overline{u}_{i,j}} \quad \text{and} \quad \beta = \tfrac{1}{2}\left(z_{j+1} - z_{j-1}\right)\left(z_{j+1} - z_j\right)\left(z_j - z_{j-1}\right) \quad , \tag{17}$$

then equation 16 can be solved for $\overline{C}_{i-1,j}$ as

$$-\frac{\alpha}{\beta}\left(z_j - z_{j-1}\right)\overline{C}_{i,j+1} + \left[1 + \frac{\alpha}{\beta}\left(z_{j+1} - z_{j-1}\right)\right]\overline{C}_{i,j} - \frac{\alpha}{\beta}\left(z_{j+1} - z_j\right)\overline{C}_{i,j-1} = \overline{C}_{i-1,j} \quad . \tag{18}$$

Here, equation 18 can be solved via the Thomas algorithm, where the input vectors **a**, **b**, **c**, and **r** are given as

$$a_{i,j} = -\frac{\alpha}{\beta}\left(z_{j+1} - z_j\right) \quad , \tag{19}$$

$$b_{i,j} = 1 + \frac{\alpha}{\beta}\left(z_{j+1} - z_{j-1}\right) \quad , \tag{20}$$

$$c_{i,j} = -\frac{\alpha}{\beta}\left(z_j - z_{j-1}\right) \quad , \tag{21}$$

and

$$r_{i,j} = \overline{C}_{i-1,j} \quad . \tag{22}$$

Figure 7 shows the two-dimensional (2-D) scalar field as computed by the steady-state model. For this example, the vertical and horizontal grid dimensions (i.e., Δz = 0.25, 0.5, 1.0 *m* and Δx = 0.5 *m*) and the initial scalar profile are the same as those described earlier in the report. In

contrast, figure 8 shows the 2-D steady-state scalar field for the case where $\Delta x = 2.0\ m$. Here, the magnitude of the horizontal grid increment is not critical because the stability criterion for this model is given as

$$\frac{1}{1+\dfrac{4K\Delta t}{(\Delta z)^2}} < 1 \quad , \tag{23}$$

where one may substitute $\Delta t = \Delta x / \overline{u}$. Thus, a simple, unconditionally stable 2-D diffusion model has been developed to test the basic formulation and correct implementation of variable grid and implicit differencing to solve the steady state scalar field.

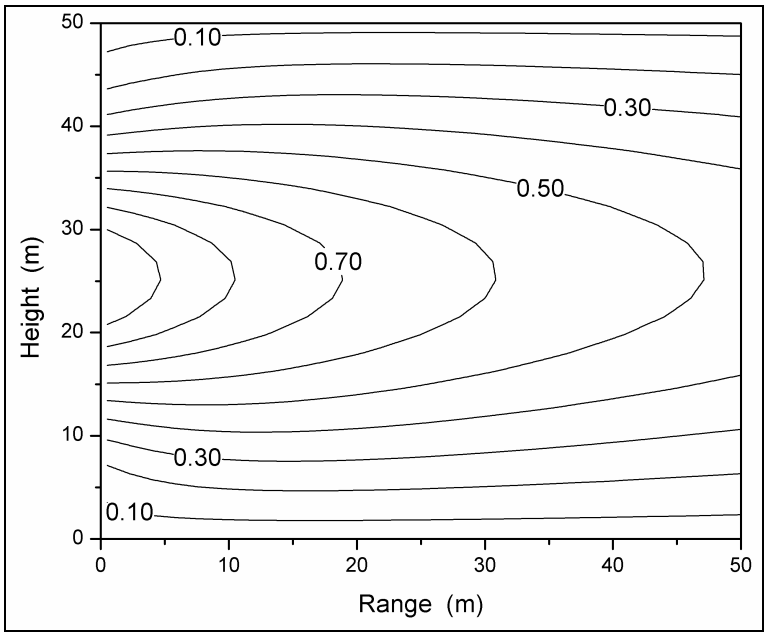

Figure 7. The 2-D steady-state scalar field derived from a scalar diffusion model solved via an implicit differencing scheme. In this example, the scalar diffusivity is $K = 10\ m^2\ s^{-1}$ and the horizontal grid is $\Delta x = 0.5\ m$.

4.2 Coupled Meteorological—Acoustic Computer Model

In this section, successful preliminary tests on simpler (diffusion) codes are extended to more complicated meteorological—acoustic models for the forest canopy. As an example, Tunick (*4*) gives the parameterized equation for Reynolds stress $\langle \overline{u'w'} \rangle$ as

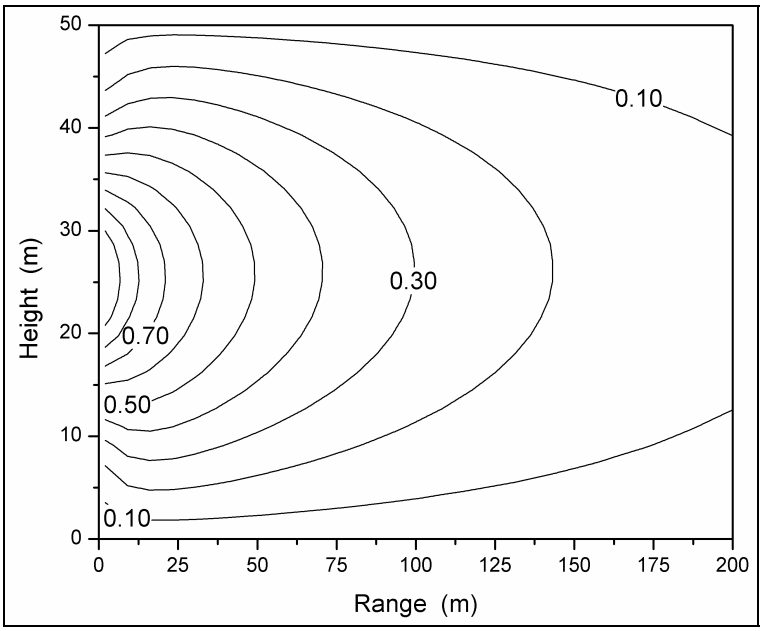

Figure 8. Same as figure 7 except the horizontal grid is $\Delta x = 2.0\ m$.

$$\frac{\partial\langle\overline{u'w'}\rangle}{\partial t} = 0 = -\langle\overline{u}\rangle\frac{\partial\langle\overline{u'w'}\rangle}{\partial x} - \langle\overline{w}\rangle\frac{\partial\langle\overline{u'w'}\rangle}{\partial z} - \langle\overline{u'w'}\rangle\frac{\partial\langle\overline{u}\rangle}{\partial x} - \langle\overline{w'^2}\rangle\frac{\partial\langle\overline{u}\rangle}{\partial z}$$
$$- \langle\overline{u'^2}\rangle\frac{\partial\langle\overline{w}\rangle}{\partial x} - \langle\overline{u'w'}\rangle\frac{\partial\langle\overline{w}\rangle}{\partial z}$$
$$+ \frac{\partial}{\partial x}\left(q\lambda_1\left(2\frac{\partial\langle\overline{u'w'}\rangle}{\partial x} + \frac{\partial\langle\overline{u'^2}\rangle}{\partial z}\right)\right) + \frac{\partial}{\partial z}\left(q\lambda_1\left(\frac{\partial\langle\overline{w'^2}\rangle}{\partial x} + 2\frac{\partial\langle\overline{u'w'}\rangle}{\partial z}\right)\right), \qquad (24)$$
$$+ \frac{g}{T}\langle\overline{u'\theta'}\rangle - \frac{q}{3\lambda_2}\langle\overline{u'w'}\rangle$$
$$+ Cq^2\left(\frac{\partial\langle\overline{u}\rangle}{\partial z} + \frac{\partial\langle\overline{w}\rangle}{\partial x}\right) + \langle\overline{w}\rangle C_d A|\overline{U}|\langle\overline{u}\rangle + \langle\overline{u}\rangle C_d A|\overline{U}|\langle\overline{w}\rangle$$

where $\langle\overline{u}\rangle$ is the mean flow – longitudinal, $\langle\overline{w}\rangle$ is the mean flow – vertical, $\langle\overline{u'^2}\rangle$ and $\langle\overline{w'^2}\rangle$ are the longitudinal and vertical velocity variances, respectively, $\langle\overline{u'\theta'}\rangle$ is the horizontal heat flux, g is the acceleration due to gravity, T is the absolute temperature, C is a constant whose value is ~0.077, q is the turbulent kinetic energy, C_d is the forest canopy drag coefficient, A (in units m^2m^{-3}) is the leaf area density, and λ is a function of mixing length.[1] The overbar and primed

[1]In equation 24, λ_1 and λ_2 are length scales, which contain two necessary closure constants, i.e., $\lambda_k = a_k l$, where k is an arbitrary index and l is the mixing length. Values for these closure constants are $a_1 = 0.39$ and $a_2 = 0.85$ (*10*).

variables indicate the mean (time averaged) and fluctuating components of the given quantity, whereas the brackets, $\langle\ \rangle$, indicate horizontal averaging. Solving equation (24) for $\partial\langle\overline{u}\rangle/\partial z$ yields

$$\begin{aligned}\left(Cq^2-\left\langle\overline{w'^2}\right\rangle\right)\frac{\partial\langle\overline{u}\rangle}{\partial z} &= \langle\overline{u}\rangle\frac{\partial\langle\overline{u'w'}\rangle}{\partial x}+\langle\overline{w}\rangle\frac{\partial\langle\overline{u'w'}\rangle}{\partial z}+\langle\overline{u'w'}\rangle\frac{\partial\langle\overline{u}\rangle}{\partial x}+\langle\overline{u'^2}\rangle\frac{\partial\langle\overline{w}\rangle}{\partial x}+\langle\overline{u'w'}\rangle\frac{\partial\langle\overline{w}\rangle}{\partial z}\\ &-\frac{\partial}{\partial x}\left(q\lambda_1\left(2\frac{\partial\langle\overline{u'w'}\rangle}{\partial x}+\frac{\partial\langle\overline{u'^2}\rangle}{\partial z}\right)\right)-\frac{\partial}{\partial z}\left(q\lambda_1\left(\frac{\partial\langle\overline{w'^2}\rangle}{\partial x}+2\frac{\partial\langle\overline{u'w'}\rangle}{\partial z}\right)\right)\\ &-\frac{g}{T}\langle\overline{u'\theta'}\rangle+\frac{q}{3\lambda_2}\langle\overline{u'w'}\rangle\\ &-Cq^2\frac{\partial\langle\overline{w}\rangle}{\partial x}-\langle\overline{w}\rangle C_d A|\overline{U}|\langle\overline{u}\rangle-\langle\overline{u}\rangle C_d A|\overline{U}|\langle\overline{w}\rangle\end{aligned} \tag{25}$$

so that

$$\frac{d\langle\overline{u}\rangle}{dz}=\frac{[\ r.h.s.\ ]}{Cq^2-\left\langle\overline{w'^2}\right\rangle}=GRADU_{i,j}\quad . \tag{26}$$

where *r.h.s.* contains all the terms on the right-hand side of equation 25. Based on this expression, the following second-order ordinary differential equation can be set up to solve for $\langle\overline{u}\rangle$, i.e.,

$$\frac{d^2\langle\overline{u}\rangle}{dz^2}=\frac{d}{dz}\left[GRADU_{i,j}\right]\ . \tag{27}$$

Equation 27 can be discretized over a variable grid as

$$\frac{\left(z_j-z_{j-1}\right)\langle\overline{u}\rangle_{i,j+1}-\left(z_{j+1}-z_{j-1}\right)\langle\overline{u}\rangle_{i,j}+\left(z_{j+1}-z_j\right)\langle\overline{u}\rangle_{i,j-1}}{0.5\left(z_{j+1}-z_{j-1}\right)\left(z_{j+1}-z_j\right)\left(z_j-z_{j-1}\right)}=\frac{GRADU_{i,j+1}-GRADU_{i,j-1}}{z_{j+1}-z_{j-1}}\quad . \tag{28}$$

Now, equation 28 can be solved via the tridiagonal matrix algorithm, where the sub-, main-, and super-diagonal vectors (**a**, **b**, and **c**, respectively) are as follows:

$$a_{i,j} = \frac{\left\langle \overline{u} \right\rangle_{i,j-1}}{0.5\left(z_{j+1} - z_{j-1}\right)\left(z_j - z_{j-1}\right)} \quad , \tag{29}$$

$$b_{i,j} = \frac{-\left\langle \overline{u} \right\rangle_{i,j}}{0.5\left(z_{j+1} - z_j\right)\left(z_j - z_{j-1}\right)} \quad , \tag{30}$$

and

$$c_{i,j} = \frac{\left\langle \overline{u} \right\rangle_{i,j+1}}{0.5\left(z_{j+1} - z_{j-1}\right)\left(z_{j+1} - z_j\right)} \quad . \tag{31}$$

Finally, the input vector **r** is given as

$$r_{i,j} = \frac{GRADU_{i,j+1} - GRADU_{i,j-1}}{z_{j+1} - z_{j-1}} \quad . \tag{32}$$

This procedure is similarly applied to solve the other 2-D meteorological fields, which include mean temperature, vertical velocity, fluctuation pressure, and heat flux.

Figure 9 shows the computed horizontal wind velocity $\left\langle \overline{u} \right\rangle$, in units ms^{-1}, over a variable grid within and above a uniform forest stand. For this example, canopy height is 10 m. In contrast, figure 10, shows the computed horizontal wind velocity, $\left\langle \overline{u} \right\rangle$, and wind flow streamlines over a variable grid within and above a non-uniform forest stand, i.e., one that contains multiple step changes in canopy height at the lower boundary.

5. Summary

Introducing variable grid will improve the efficiency and realism of coupled meteorological—acoustic computer models. Variable grid will allow for better distribution of grid points and will extend calculations higher into the boundary layer above the forest. A finer grid inside the forest and a coarser grid above the forest will help to resolve important meteorological (and acoustic) scales and processes. Therefore, this report has presented results from some preliminary tests to incorporate variable grid into current software. Several basic model codes were developed to benchmark the fundamental (numerical) techniques, i.e., to solve diffusion equations via explicit and implicit differencing. These calculations worked quite well. In addition, numerical stability criteria for these calculations were clearly demonstrated.

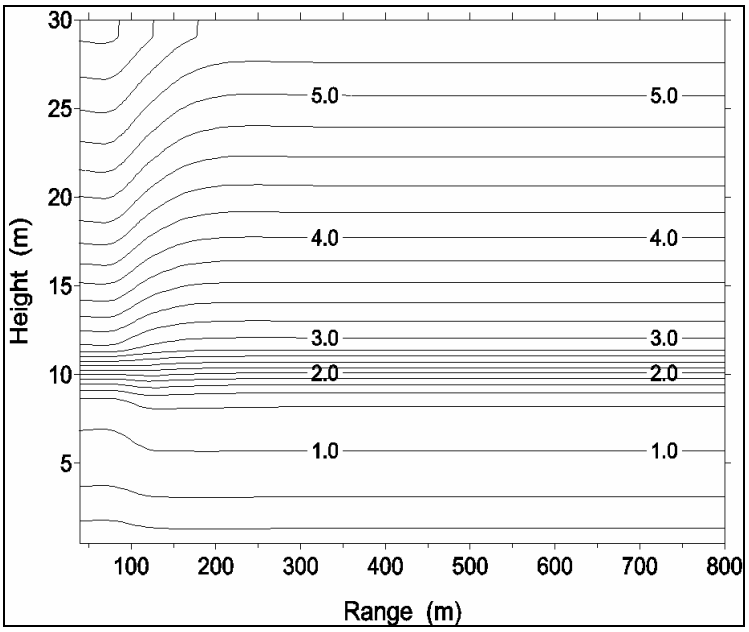

Figure 9. Horizontal wind velocity, $\langle \bar{u} \rangle$, in units ms^{-1}, within and above a uniform forest stand, where canopy height (h) is 10 m.

Although difficult to perform, stability analysis is important so that models will be computationally robust. In this report, it was shown that the magnitude of the time-step (and/or horizontal grid increment) was not critical for the time-dependent and steady-state diffusion models solved via implicit differencing. However, in current meteorological—acoustic software, the stable calculation of the second horizontal derivatives (as well as the mixed derivatives) is found to necessitate fairly large Δx (e.g., 30-50 m). Hence, further analysis and interpretation of model results are in progress to resolve some remaining difficulties in establishing a finer (horizontal) grid in existing meteorological—acoustic codes.

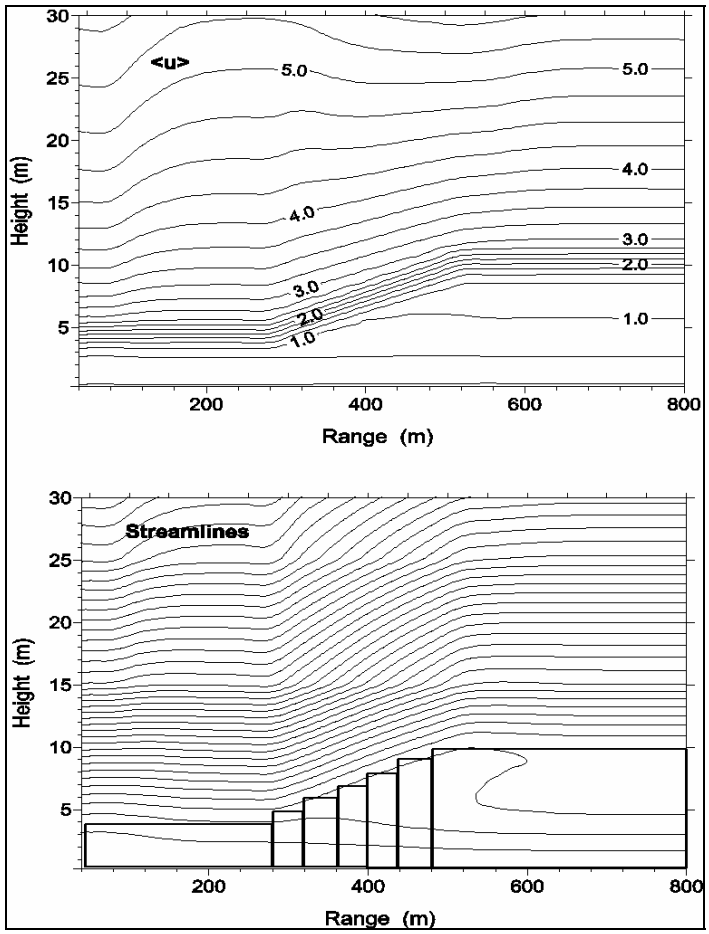

Figure 10. Horizontal wind velocity, $\langle \bar{u} \rangle$, in units ms^{-1}, and the wind flow streamlines within and above a non-uniform forest stand, i.e., one that contains multiple step changes in canopy height (h) at the lower boundary.

6. References

1. Srour, N. Army Acoustics Needs. Sensor Arrays, Distributed Sensors and Applications. *DARPA Air-Coupled Acoustic Micro Sensors Workshop*, Crystal City, VA, 24–25 August 1999.

2. Wilson, D. K. *A Prototype Acoustic Battlefield Decision Aid Incorporating Atmospheric Effects and Arbitrary Sensor Layouts*; ARL-TR-1708; U.S. Army Research Laboratory: Adelphi, MD, 1998.

3. Tunick, A. Calculating the Micrometeorological Influences on the Speed of Sound Through the Atmosphere in Forests. *Journal of the Acoustical Society of America*. **2003**, *114*, 1796–1806.

4. Tunick, A. *A Two-Dimensional Meteorological Computer Model for the Forest Canopy*; ARL-MR-569; U.S. Army Research Laboratory: Adelphi, MD, 2003.

5. Ferziger, J. H.; Perić, M. *Computational Methods for Fluid Dynamics;* 3rd Ed.; Springer-Verlag: Berlin, 2002.

6. Munn, R. E. *Descriptive Micrometeorology*; Academic Press: New York, 1966.

7. Press, W. H.; Teukolsky, S. A.; Vetterling, W. T.; Flannery, B. P. *Numerical recipes in Fortran*; 2nd Ed.; Cambridge University Press: New York, 1992; p 838.

8. Press, W. H.; Teukolsky, S. A.; Vetterling, W. T.; Flannery, B. P. *Numerical recipes in Fortran*; 2nd Ed.; Cambridge University Press: New York, 1992; p 42.

9. Press, W. H.; Teukolsky, S. A.; Vetterling, W. T.; Flannery, B. P. *Numerical recipes in Fortran*; 2nd Ed.; Cambridge University Press: New York, 1992; p 840.

10. Katul, G. G.; Albertson, J. D. An Investigation of Higher-Order Closure Models for a Forested Canopy. *Boundary-Layer Meteorology*, **1998**, *89*, 47–74.

Distribution

Admnstr
Defns Techl Info Ctr
ATTN DTIC-OCP (Electronic Copy)
8725 John J Kingman Rd Ste 0944
FT Belvoir VA 22060-6218

DARPA
ATTN IXO S Welby
3701 N Fairfax Dr
Arlington VA 22203-1714

US Military Acdmy
Mathematical Sci Ctr of Excellence
ATTN LTC T Rugenstein
Thayer Hall Rm 226C
West Point NY 10996-1786

Sci & Technlgy Corp
10 Basil Sawyer Dr
Hampton VA 23666-1340

US Army CRREL
ATTN CECRL-GP M Moran
ATTN CERCL-SI E L Andreas
72 Lyme Rd
Hanover NJ 03755-1290

US Army Dugway Proving Ground
DPG Meteorology Div
ATTN J Bowers
West Desert Test Center
Dugway UT 84022-5000

Nav Postgraduate Schl
Dept of Meteorology
ATTN P Frederickson
1 University Cir
Monterey CA 93943-5001

Air Force
ATTN Weather Techl Lib
151 Patton Ave Rm 120
Asheville NC 28801-5002

Colorado State Univ
Dept of Atmos Sci
ATTN R A Pielke
200 West Lake Street
FT Collins CO 80523=□-1371

Duke Univ Pratt Schl of Engrg
Dept of Civil & Environ Engrg
ATTN R Avissar
Hudson Hall-Box 90287
Durham NC 27708

The City College of New York
Dept of Earth & Atmos Sci
ATTN S D Gedzelman
J106 Marshak Bldg 137th and Convent Ave
New York City NY 10031

Univ of Alabama at Huntsville
Dept of Atmos Sci
ATTN R T Mcnider
Huntsville AL 35899

Natl Ctr for Atmos Rsrch
ATTN NCAR Library Serials
PO Box 3000
Boulder CO 80307-3000

Director
US Army Rsrch Lab
ATTN AMSRD-ARL-RO-D JCI Chang
ATTN AMSRD-ARL-RO-EN W D Bach
PO Box 12211
Research Triangle Park NC 27709

US Army Rsrch Lab
ATTN AMSRD-ARL-D J M Miller
ATTN AMSRD-ARL-SE J Pellegrino
ATTN AMSRD-ARL-CI J D Gantt
ATTN AMSRD-ARL-CI-IS Mail &
Records Mgmt
ATTN AMSRD-ARL-CI-OK-T
Techl Pub (2 copies)
ATTN AMSRD-ARL-CI-OK-TL
Techl Lib (2 copies)

US Army Rsrch Lab (cont'd)
ATTN AMSRD-ARL-CI-EE P Clark
ATTN AMSRD-ARL-SE-SA N Srour
ATTN AMSRD-ARL -CI-CS R Meyers
ATTN AMSRD-ARL -SE-EE
Z G Sztankay
ATTN AMSRD-ARL-CI-EE
A Tunick (15 copies)
Adelphi, MD 20783-1197